論　文

Impact of TiB$_2$ Particle Size Distribution on Grain Refining Effectiveness*

Akihiro Minagawa**

Grain refiners of the Al-Ti-B system, including TiB$_2$ particles, are added to molten aluminum to produce the fine grains. The effect of grain refinement effectiveness varies among grain refiner manufacturers and the lots despite the same chemical content. It is unclear which parameters vary the grain refinement effectiveness. Many studies suggest that the fine grains are achieved by grain refiner due to the TiB$_2$ particles act as heterogeneous nuclei. The free growth model is a famous model for the grain refinement. This model assumes that the TiB$_2$ particle size distribution influences the inoculation efficiency. However, there are few examples that verified the inoculation efficiency using grain refiners with different TiB$_2$ particle size distributions. In this study, the effect of TiB$_2$ particle size distribution and chemical content for grain refinement effectiveness was investigated by using several grain refiners. The TiB$_2$ particle size distribution in the grain refiner was measured by image analysis and applied to the grain size prediction model which was developed based on the free growth model. The experimental and calculated results were compared and discussed in order to clarify whether the new model can predict the grain size of cast sample with each grain refiner.

Keywords: *grain refiner, grain refinement, boride, agglomeration*

1. Introduction

For the aluminum DC casting, the Al-Ti-B system grain refiner is generally used to achieve a fine grain structure. The grain refiner is an important material because it determines the ingot quality. However, the mechanism of grain refinement by grain refiner is not understood completely. Many studies have proposed that the TiB$_2$ particles in the grain refiner act as heterogeneous nuclei. However, the actual inoculation efficiency is very low (approximately 1%). Moreover, the inoculation efficiency significantly varies with the grain refiner manufacturers and the lots despite the same chemical content.

Many studies have tried to clarify these phenomena[1]~[7]. Greer et al.[1] proposed a free growth model in which all grains grow through inoculated TiB$_2$ particles. This model explains that nucleation will preferentially occur from large TiB$_2$ particles. The TiB$_2$ particle size distribution is an important factor in predicting the inoculation efficiency.

However, there are few experimental results using several grain refiners with different TiB$_2$ particle size distributions. In addition, this model cannot use multiple values of the liquidus slope m and the equilibrium partition k. It should be modified to apply various alloys. Vainik et al.[8] found that the dispersion state of the TiB$_2$ particles in the molten aluminum also affects the inoculation efficiency. These reports used only Al-5Ti-1B (mass%, following is same) refiners, but it is still unclear whether other kind of grain refiner show the same trend.

In this study, the grain refinement effectiveness of several grain refiners with different manufacturers and chemical contents was investigated. The main part of TiB$_2$ particles in the grain refiner are agglomerates. Therefore, the TiB$_2$ particle size distributions of each grain refiner were measured as individual particle and agglomerates to verify the effect of agglomeration. A new grain size prediction model, which is a modified free growth model, was developed due to apply various alloy parameters.

Finally, the effect of the TiB₂ particle size distribution and agglomeration on the inoculation efficiency was discussed by experiment and calculation results.

2. Experimental Method

In this study, Al-5Ti-1B and Al-5Ti-0.2B (mass%, following is same) from manufacturers A and B were used in the grain refinement test. **Table 1** shows the chemical content of the pure aluminum before adding each refiner. These data are the results of an emission spectroscopic analysis. About 5 kg of pure aluminum was melted in an electric furnace and maintained in the range of 988-998 K. The grain refiner was added to the melt at 0.2, 0.1, and 0.05% and melt was stirred for 30 seconds. After stirring, the melt was held for 90 seconds, and then cast. The casting equipment is the same as used in the TP1 test[9]. The cross section at a position 38 mm from the lower end of the ingot was observed using a microscope. The average grain size was measured by the planimetric method.

3. Grain Size Prediction Model

The modified grain size prediction model is based on the free growth model[1]. The free growth model assumes that free growth of a grain begins on a TiB₂ particle with undercooling inversely proportional to the diameter of the TiB₂ particle. The nucleation undercooling is not considered because they are very small with TiB₂ particle[10]. The minimum undercooling $\Delta T_{\min}$ required to start the free growth is given by

$$\Delta T_{\min} = \frac{2\sigma}{\Delta S_{V} r^{*}} \tag{1}$$

where ΔS_{V} is the entropy of fusion per unit, σ is the solid-liquid interfacial energy, and r^{*} is the critical embryo radius. According to the invariant-size

approximation model[11], which was proposed for the diffusion controlled growth of a spherical precipitate of radius in a solid matrix, the radius of a spherical particle r is given by

$$r = \lambda (D \cdot t)^{1/2} \tag{2}$$

and differentiating equation (2) with respect to time gives the growth rate of the spherical crystals as

$$V = \frac{dr}{dt} = \frac{\lambda^{2} D}{2r} \tag{3}$$

where V is the growth rate, D is the solute diffusion coefficient in the liquid and t is the time. λ is an interfacial parameter and obtained from the interface content profiles[11]

$$\lambda = \left(\frac{-S}{2\pi^{1/2}}\right) + \left(\frac{S^{2}}{4\pi} - S\right)^{1/2} \tag{4}$$

in which

$$S = \frac{2(C_{IL} - C_{0})}{(C_{IS} - C_{IL})} \tag{5}$$

where C_{IL} and C_{IS} are the solute content in the liquid and the solid, respectively, at the solid-liquid interface. C_{0} is the solute content in the melt alloy. S can vary between -2 and 0[3]. The solute undercooling ΔT_{s} is given by

$$\Delta T_{s} = m(C_{0} - C_{IL}) \tag{6}$$

where m is the liquidus slope. Substituting Eq. (6) and the equilibrium partition coefficient $k = C_{IS} / C_{IL}$, Eq. (5) becomes

$$S = -2 \cdot \frac{\Delta T_{s}}{m(k-1)(C_{0} - \Delta T_{s} / m)} \tag{7}$$

when using Eq. (7), only one solute parameter can be

Table 1 Chemical content of each condition before adding the grain refiner.

Grain refiner		Chemical composition / %			
Manufacturer	Composition Ti / B	Fe	Si	V	Ti
A	5/1	0.07	0.03	0.02	0.0049
	5/0.2	0.08	0.03	0.01	0.0045
B	5/1	0.09	0.03	0.01	0.0045
	5/0.2	0.08	0.03	0.01	0.0045

used. Thus, the approximation proposed by Qian et al.[6] was applied. When spherical crystal is small, in addition to ΔT_s, it is necessary to consider the curvature undercooling ΔT_c. Qian et al assumed that ΔT_s will be large enough to ignore ΔT_c when the nucleation occurs. Therefore, when $\Delta T_s = \Delta T$, Eq. (7) gives

$$S = -2 \cdot \frac{\Delta T}{m(k-1)(C_0 - \Delta T/m)} \tag{8}$$

ΔT is the overall melt undercooling. In most cases, ΔT is very small with TiB₂ particle and $\Delta T/m$ can be ignored. Consequently, Eq. (8) becomes

$$S \approx -2\frac{\Delta T}{Q} \tag{9}$$

in which

$$Q = m(k-1)C_0 \tag{10}$$

where Q is termed the growth-restriction parameter. By using parameter Q, it is possible to consider m and k of all solute content. Furthermore, where ΔT is very small (< 1 K) and Q values are an order of magnitude larger than ΔT. That means $|S| \ll 1$ and Eq. (4) simplified to

$$\lambda \approx (-S)^{1/2} = \left(\frac{2\Delta T}{Q}\right)^{1/2} \tag{11}$$

Therefore, the growth rate of the spherical crystals becomes

$$V = \frac{\Delta T D}{rQ} \tag{12}$$

The calculation process is the same as Greer's free growth model. The temperature decreases at each time step according to the set cooling rate. Each particle will grow with the rate calculated by Eq. (12) if the melt temperature reaches or exceeds the minimum undercooling. Latent heat will be calculated depending on the increase of solid volume. The rising temperature on each time step is the latent heat divided by the specific heat. **Table 2** and **Table 3** show the physical property values and the solute element parameters used in calculations respectively. The cooling rate is 6.4 K/s, which is the average value obtained from four experiments. The TiB₂ particle size distributions were measured from SEM image of each grain refiner by image analysis. In order to investigate the relationship between the inoculation efficiency and the aggregation state of the TiB₂ particles in the grain refiner, TiB₂ particle size distributions were measured by two methods. Prior to the particle analysis, one TiB₂ particles were not treated and the other was manually divided into individual TiB₂ particles. Four SEM images of each refiner were used for the image analysis. In order to avoid confusion with polished scratches, particles smaller than 0.3 µm were excluded from the measurement. **Fig. 1** shows SEM images and result of particle measurement analysis. **Fig. 2** shows particle size distributions of each grain refiner. From these results, it was confirmed that the particle size distributions in each grain refiner was different.

Table 2　The material parameters used in the calculation[1].

Physical property value	Symbol	Units	Value
Solid-liquid interfacial energy	σ	mJ/m²	158
Entropy of fusion per unit volume	ΔS_V	J/K m³	1.112×10^6
Enthalpy of fusion per unit volume	ΔH_V	J/m³	9.5×10^8
Heat capacity of melt per unit volume	C_{PV}	J/K m³	2.58×10^6
Diffusivity in melt (Ti in Al)	D_S	m²/s	2.52×10^{-9}

Table 3　The solute element parameters used in the calculation[1].

Solute element	$m/\text{K}\cdot\text{s}^{-1}$	$k/-$
Fe	−2.93	0.03
Si	−6.62	0.12
V	9.71	3.33
Ti	25.63	7.00

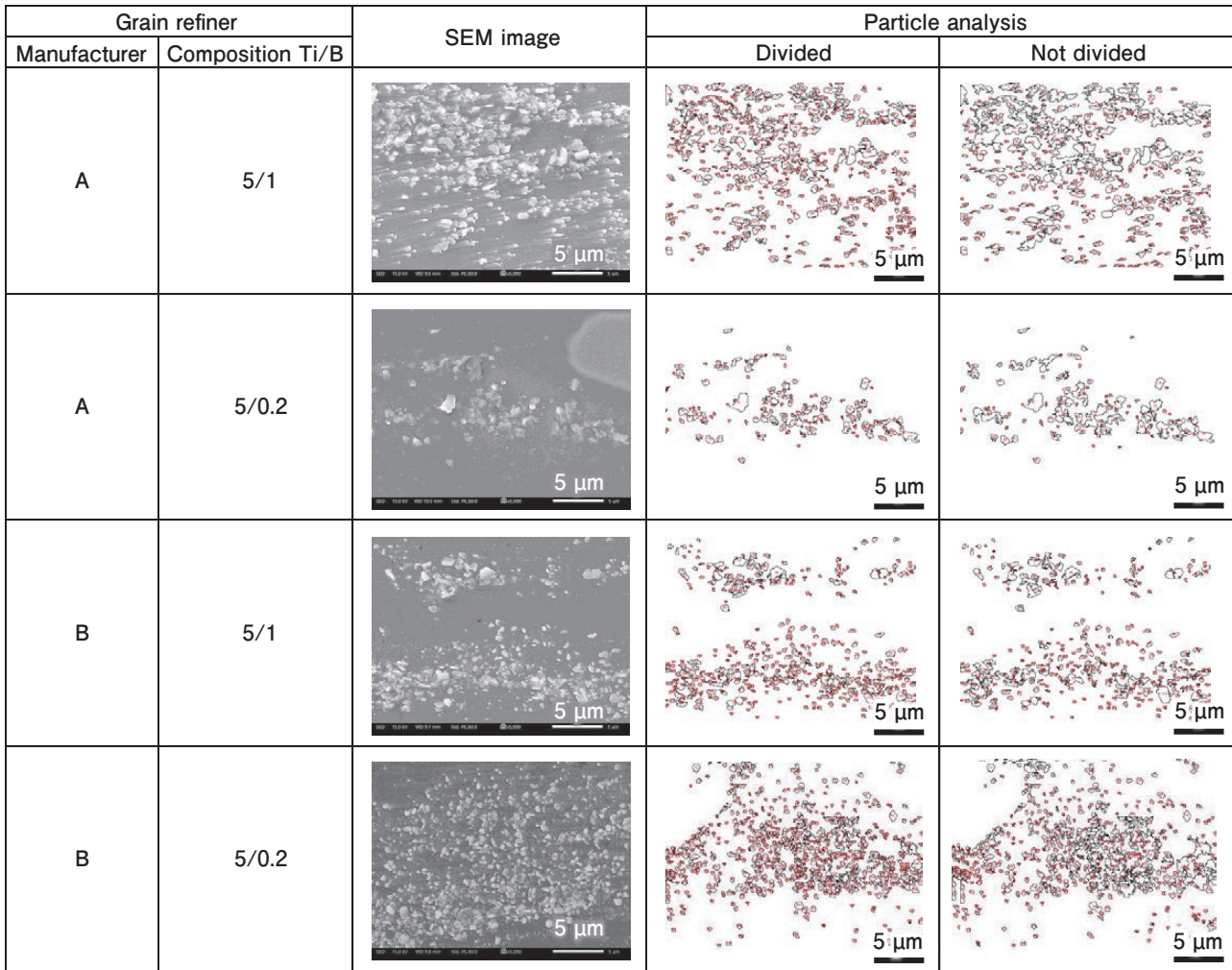| Grain refiner		SEM image	Particle analysis	
Manufacturer	Composition Ti/B		Divided	Not divided
A	5/1			
A	5/0.2			
B	5/1			
B	5/0.2			

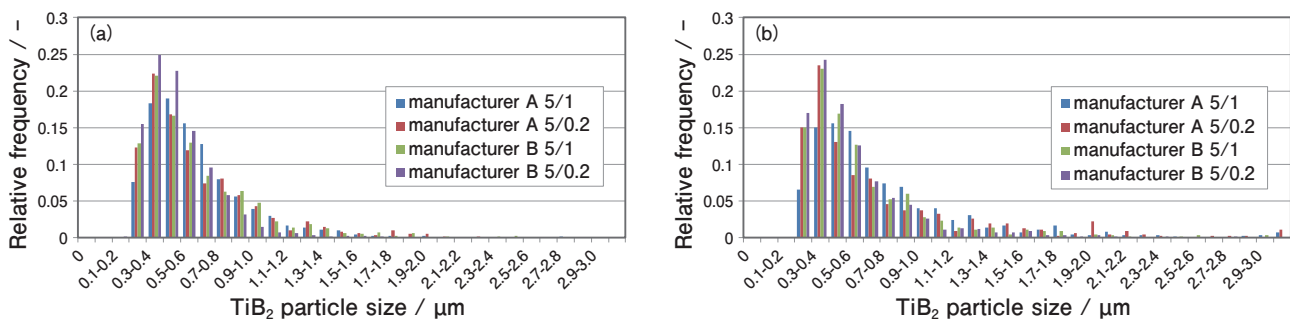**Fig. 1** SEM images and results of particle analysis.

Fig. 2 TiB₂ particle size distribution (a: divided particle, b: not divided particle).

4. Results

Fig. 3 shows the results of the grain refinement tests. The horizontal axis is the target content of the titanium and the vertical axis is the grain size. When Al-5Ti-0.2B was added, there was no difference in the grain size between manufacturers. On the other hand, manufacturer B's Al-5Ti-1B refiner showed poor grain refinement efficiency compared with manufacturer

A's refiner. The grain sizes of cast sample with Al-5Ti-0.2B were larger than it with Al-5Ti-1B. **Fig. 4** shows the relationship between the grain size and titanium content. The titanium content is the increments before and after adding the grain refiner obtained by spark optical emission spectroscopic analysis. When manufacturer A's refiner was added, there was a difference in the relationship between the titanium content and grain size due to the difference

in the chemical content. On the other hand, when manufacturer B's refiner was added, the grain size decreased with the increasing titanium amount regardless of the chemical content. **Fig. 5** shows the relationship between the grain size and boron
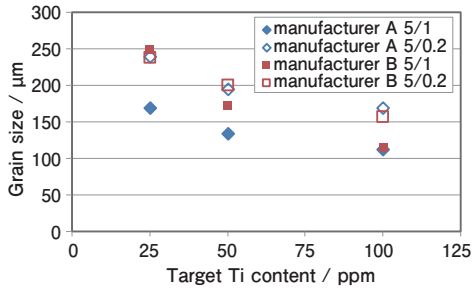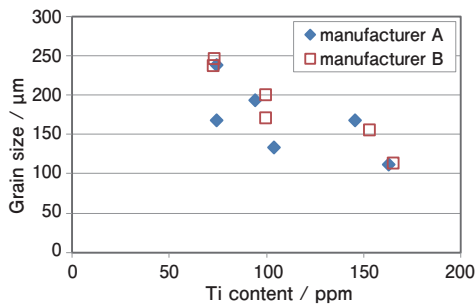

Fig. 3   Grain refinement test results.

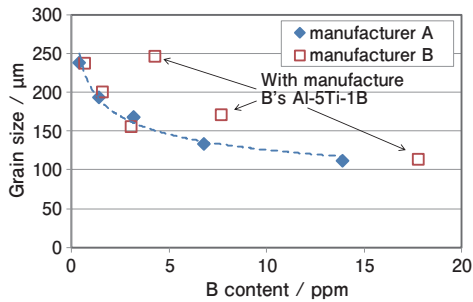**Fig. 4**   Relationship between grain size and titanium content.

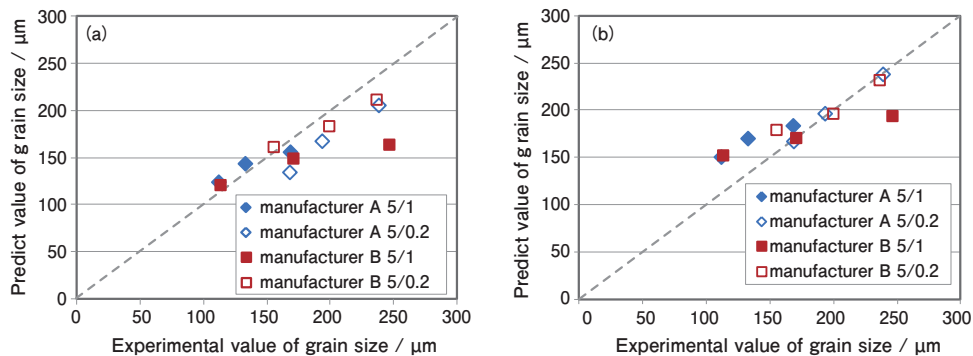**Fig. 5**   Relationship between grain size and boron content.

content. The boron content is the increments before and after adding the grain refiner. Regardless of the chemical content and manufacturer, the grain size was refined with the increasing boron content, except for manufacturer B's Al-5Ti-1B.

Fig. 6 compares the grain size between the grain refinement test and calculations. The horizontal axis is the grain size obtained by the experiment and the vertical axis is the grain size obtained by the calculations. Regardless of the particle size distribution measurement method, the results of the experiments using manufacturer B's Al-5Ti-1B deviated from the calculation results. When Al-5Ti-0.2B was added, the experimental results well agreed with the calculation results using the undivided TiB₂ particle size distribution. When manufacturer A's Al-5Ti-1B was added, the experimental results well agreed with the results calculated using the divided TiB₂ particle size distribution.

5. Discussion

The grain size of the samples with Al-5Ti-0.2B was larger than that of the sample with Al-5Ti-1B. In addition, the grain size will be fined with the increasing boron except for manufacturer B's Al-5Ti-1B. Therefore, even if the chemical content of grain refiner is different, the amount of TiB₂ is considered to be main factor affecting on grain refinement effectiveness.

Even when the agglomerated TiB₂ particle size distribution was used in the prediction model, the experimental and calculated results almost agreed. Especially, it showed good agreement when Al-5Ti-0.2B was used. Therefore, the TiB₂ agglomerates in

Fig. 6   Comparison of grain size between experiment and calculations (a: divided particle, b: not divided particle).

the grain refiner were estimated that it will not be broke-up in the molten aluminum. Furthermore, it was suggested that the break up behavior is different depending on the chemical content of grain refiner. For that reason, it was estimated that the accuracy of the prediction model will improve if the break up behavior is clarified.

The reason why manufacturer B's refiner showed poor grain refinement effectiveness was not explained by the TiB_2 particle size distribution. Therefore, it is suggested that the affecting factor of the grain refinement effectiveness is not only the TiB_2 particle size distribution. When the addition rate of manufacturer B's refiner was low, predicted value was smaller than experimental value. It indicates that the TiB_2 particle sizes, which act as heterogeneous nuclei in the calculation, were smaller than in the experiment. In this model, the growth restriction effect by solute content was overestimated by applying various approximations. Furthermore, the undercooling[12] depending on the curvature of nucleated grain on TiB_2 particle was ignored. Therefore, the predicted value tends to show lower value. In the future, the effect of curvature should be added to this model to improve accuracy.

6. Conclusion

1. Regardless of the grain refiner component, the grain size was changed based on the amount of TiB_2.

2. The difference in the TiB_2 particle size distribution couldn't explain the significant difference in the grain refinement effect.

3. The calculated and experimental results were in good agreement except for the condition using the grain refiner with low refinement efficiency.

4. When the agglomerated TiB_2 particle distribution was used in the prediction model, the experimental results with Al-5Ti-0.2B grain refiner and the calculated results showed good agreement. Therefore, it was suggested that the TiB_2 agglomerates in the grain refiner will not be broke up in the molten aluminum.

Acknowledgment

REFERENCES

1) A.L. Greer, A.M. Bunn, A. Tronche, P.V. Evans and D.J. Bristow: Acta Mater., **48** (2000), 2823-2835.

2) A.M. Bunn, P.V. Evans, D.J. Bristow and A.L. Greer: Light Metals 1998 ed. by B. Welch, (1998), 963-968.

3) I. Maxwell and A. Hellawell: Acta Metall., **23** (1975), 229-237.

4) D.H. StJohn, M. Qian, M.A. Easton and P. Cao: Acta Mater., **59** (2011), 4907-4921.

5) M.A. Easton and D.H. StJohn: Mater. Sci. Eng. A, **486** (2008), 8-13.

6) M. Qian, P. Cao, M.A. Easton, S.D. McDonald and D.H. StJohn: Acta Mater., **58** (2010), 3262-3270.

7) W. Dai, X. Wang, W. Zhao and Q. Han: Light Metals 2014 ed. by J. Grandfield, (2014), 945-949.

8) R. Vainik, L. Backerud and J. Courtenay: Light Metals 2006 ed. by T.J. Galloway, (2006), 789-791.

9) Standard Test Procedure for Aluminum Alloy Grain Refiners 2012, The Aluminum Association, (2012).

10) A. Prasad, S.D. McDonald, H. Yasuda, K. Nogita and D.H. StJohn: J. Cryst. Growth, **430** (2015), 122-137.

11) H.B. Aaron, D. Fainstein and G.R. Kotler: J. Appl. Phys., **41** (1970), 4404-4410.

12) J.A. Dantzig and M. Rappaz: EPFL Press, Switzerland (2016).

Akihiro Minagawa

Research Department II,
Research & Development Division,
UACJ Corporation